HRP2 Determines the Efficiency and Specificity of HIV-1 Integration in LEDGF/p75 Knockout Cells but Does Not Contribute to the Antiviral Activity of a Potent LEDGF/p75-Binding Site Integrase Inhibitor

11518–11530 *Nucleic Acids Research, 2012, Vol. 40, No. 22* *Published online 5 October 2012*
doi:10.1093/nar/gks913

HRP2 determines the efficiency and specificity of HIV-1 integration in LEDGF/p75 knockout cells but does not contribute to the antiviral activity of a potent LEDGF/p75-binding site integrase inhibitor

Hao Wang[1], Kellie A. Jurado[1], Xiaolin Wu[2], Ming-Chieh Shun[1], Xiang Li[1], Andrea L. Ferris[3], Steven J. Smith[3], Pratiq A. Patel[4], James R. Fuchs[4], Peter Cherepanov[5], Mamuka Kvaratskhelia[6], Stephen H. Hughes[3] and Alan Engelman[1,*]

[1]Department of Cancer Immunology and AIDS, Dana-Farber Cancer Institute and Department of Medicine, Harvard Medical School, Boston, MA 02215, USA, [2]Laboratory of Molecular Technology, SAIC-Frederick Inc., [3]HIV Drug Resistance Program, Frederick National Laboratory for Cancer Research, Frederick, MD 21702, USA, [4]Division of Medicinal Chemistry and Pharmacognosy, College of Pharmacy, The Ohio State University, Columbus, OH 43210, USA, [5]Clare Hall Laboratories, London Research Institute, Cancer Research UK, Hertfordshire, EN6 3LD UK and [6]Center for Retrovirus Research and Comprehensive Cancer Center, College of Pharmacy, The Ohio State University, Columbus, OH 43210, USA

Received July 30, 2012; Revised September 6, 2012; Accepted September 9, 2012

ABSTRACT

The binding of integrase (IN) to lens epithelium-derived growth factor (LEDGF)/p75 in large part determines the efficiency and specificity of HIV-1 integration. However, a significant residual preference for integration into active genes persists in *Psip1* (the gene that encodes for LEDGF/p75) knockout (KO) cells. One other cellular protein, HRP2, harbors both the PWWP and IN-binding domains that are important for LEDGF/p75 co-factor function. To assess the role of HRP2 in HIV-1 integration, cells generated from *Hdgfrp2* (the gene that encodes for HRP2) and *Psip1*/*Hdgfrp2* KO mice were infected alongside matched control cells. HRP2 depleted cells supported normal infection, while disruption of *Hdgfrp2* in *Psip1* KO cells yielded additional defects in the efficiency and specificity of integration. These deficits were largely restored by ectopic expression of either LEDGF/p75 or HRP2. The double-KO cells nevertheless supported residual integration into genes, indicating that IN and/or other host factors contribute to integration specificity in the absence of LEDGF/p75 and HRP2. *Psip1* KO significantly increased the potency of an allosteric inhibitor that binds the LEDGF/p75 binding site on IN, a result that was not significantly altered by *Hdgfrp2* disruption. These findings help to rule out the host factor-IN interactions as the primary antiviral targets of LEDGF/p75-binding site IN inhibitors.

INTRODUCTION

Reverse transcription of genomic RNA and the subsequent integration of viral DNA are essential events in retroviral replication. The key cutting and joining steps of the integration reaction are catalysed by the viral-encoded integrase (IN) and carried out in the context of the viral preintegration complex (PIC). IN processes the 3′ ends of linear viral DNA adjacent to conserved CA dinucleotides, and then joins the recessed 3′ viral DNA ends to the 5′-phosphates of a staggered cut in chromosomal DNA (1,2). Cellular enzymes repair the gapped recombination intermediate to yield the integrated provirus, which is flanked by a short sequence duplication generated by the cut in the target DNA. PICs extracted from acutely infected cells support the integration of retroviral DNA into exogenous target DNA *in vitro* (1–4).

Retroviral integration is non-random, and different types of viruses display different preferences for chromatin [reviewed in (5)]. Lentiviruses such as HIV-1 integrate within transcriptionally active genes while the integration of the gammaretrovirus Moloney murine leukemia virus (MLV) favors the promoter regions of genes (6,7). Other viruses, including alpharetroviruses (8,9) and deltaretroviruses (10), show a much weaker preference for chromatin features compared with the lentiviruses

*To whom correspondence should be addressed. Tel: +1 617 632 4361; Fax: +1 617 4338; Email: alan_engelman@dfci.harvard.edu

or MLV, retaining a slight preference for promoter regions. Although the mechanisms that underlie integration site selection for most types of retroviruses are unknown, the tendency of lentiviruses, including HIV-1, to integrate within active genes is, in large part, determined by the binding of the IN protein to lens epithelium-derived growth factor (LEDGF)/p75 [reviewed in (11,12)]. The efficiency of HIV-1 integration is reduced in cells depleted for LEDGF/p75 by RNA interference (RNAi) (13,14) or gene knockout (KO) (15–18). In the absence of LEDGF/p75, the distribution of the residual proviruses trends away from active genes and shows a modest shift toward promoter regions (15,17–19). However, even in cells that completely lack LEDGF/p75, the distribution of the proviruses is significantly different from random, suggesting that other host factors might be involved in determining the specificity of HIV-1 integration.

LEDGF/p75 functions as a bimodal tether during HIV-1 integration. An N-terminal PWWP domain and two nearby copies of the AT-hook DNA-binding motif bind chromatin (20–22) whereas the C-terminally located IN-binding domain (IBD) binds IN (23–25). LEDGF/p75 is one of six members of the hepatoma-derived growth factor (HDGF) related protein (HRP) family, which is defined by similarity in the sequences of the conserved PWWP domain (23,26). One other HRP family member, HRP2, contains an IBD that is analogous to the IBD in LEDGF/p75 (23,24). Akin to LEDGF/p75, purified HRP2 protein stimulates the DNA-strand transfer activity of recombinant HIV-1 IN protein (23) and restores integration activity to salt-depleted HIV-1 PICs (27) *in vitro*, which suggests that HRP2 might play a role in integration in infected cells. Knockdown of human HRP2 (hHRP2) in cell lines has however failed to reveal a role for this IN-binding factor in HIV-1 infection (13,18,27). Co-depletion of HRP2 and LEDGF/p75 has yielded mixed results. Human T cells that support a minimal level of HIV-1 infection (about 3%) due to a prior LEDGF/p75 knockdown failed to reveal a role for HRP2 when it was subsequently knocked down (13). KO of *PSIP1*, the gene that encodes LEDGF/p75, in a human B cell line conferred an ~5-fold infection defect in viral titer, which was further reduced about 2-fold by HRP2 knockdown (18). We and others previously characterized HIV-1 infection and integration defects using mouse embryo fibroblast (MEF) cells derived from *Psip1* KO animals (15–17,22). To analyse the role of HRP2 in HIV-1 infection and integration under the stringent condition of gene KO, we generated MEF cells from mice disrupted for the *Hdgfrp2* gene, which encodes for HRP2, as well as *Hdgfrp2*/*Psip1* double-KO mice, and compared the ability of these cells to support HIV-1 integration to cells derived from littermate matched controls. Whereas *Hdgfrp2* KO cells supported normal levels of HIV-1 infection, both viral titer and integration efficiency were reduced in double-KO cells compared with single *Psip1* KO cells. The additional integration defect seen in the double-KO cells correlated with a reduction in targeting to active genes and to a loss of PIC activity *in vitro*. Moreover, ectopic expression of HRP2 compensated for the loss of LEDGF/p75 function under these conditions. An allosteric IN inhibitor (ALLINI) that targets the LEDGF/p75 binding cleft in the dimer interface of the IN catalytic core domain (CCD) (28,29) is significantly more potent when LEDGF/p75 is knocked out, effects that are not significantly altered by HRP2 depletion in either wild type (WT) or *Psip1* KO cells. Our results show that HRP2 plays a role in HIV-1 PIC function when LEDGF/p75 is absent, and rule out members of the HRP protein family as the primary antiviral targets of LEDGF/p75-binding site ALLINIs during integration.

MATERIALS AND METHODS

DNA constructs

The animal cell expression vector pIRES2-eGFP, and pIRES2-hLEDGF-HA-eGFP derivative that expresses human LEDGF/p75 [hLEDGF/p75 fused to a C-terminal hemagglutinin (HA) tag], was previously described (15). PCR-amplified full-length hHRP2-HA and mHRP2-HA (see Supplementary Table S1 for a list of primers used in this study), as well as hHRP2 lacking the 5′ end region corresponding to the PWWP domain, were introduced into pIRES2-eGFP. The plasmid pIRES2-hHRP2-HA-eGFP was mutagenized to change the Asp489 GAC codon to AAC. The pGEX-4T-1-based bacterial plasmids that express the IBDs of hLEDGF/p75 (residues 347-471) and hHRP2 (residues 470-593) fused to the C-terminus of glutathione *S*-transferase (GST) were previously described (23). The corresponding region of mHRP2 was PCR-amplified and inserted into pGEX-4T-1. All PCR-amplified regions of DNA constructs were verified by dideoxy sequencing.

Protein expression, purification and GST pull-down assay

GST fusion proteins and His_6-tagged HIV-1 IN were expressed and purified from *Escherichia coli* as previously described (23,30). The conditions for the GST pull-downs were as previously described (30).

Animal cells

HEK293T cells and primary MEFs isolated from 13.5-day post-cotium embryos were maintained in Dulbecco's modified Eagle's medium supplemented to contain 10% fetal calf serum, 100 IU/ml penicillin and 100 µl/ml streptomycin. MEF cells were transformed by expressing the simian virus (SV) 40 large T antigen as described previously (31). Cell proliferation was quantified using the cell titer kit from Promega.

DNA prepared from MEF cells using the QIAamp DNA Mircro kit (Qiagen) was genotyped using primers AE3747/AE3748, which yield a 433 bp gene trap-specific product, and AE2511/AE2512, which yield a 535 bp fragment from the third intron of the *Hdgfrp2* gene; the gene trap insertion prevents the amplification of this latter product (Figure 1A). Detection of WT and deleted *Psip1* alleles using primers AE2331/AE2802 was described previously (15). PCR mixtures contained 100 ng DNA, 0.5 µM primers, 0.2 mM of each dNTP, 2 mM $MgCl_2$ and 2.5 U Amplitaq polymerase in buffer supplied

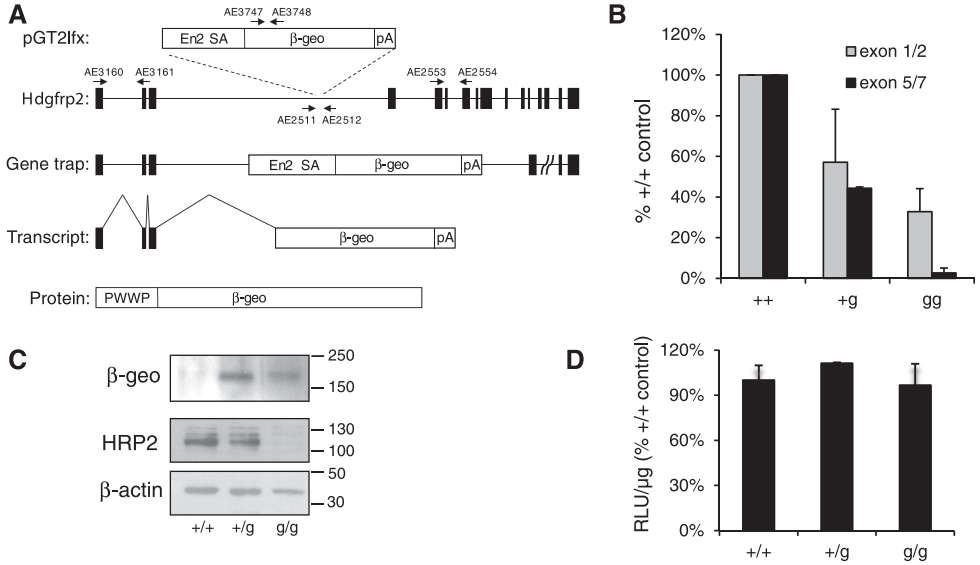

Figure 1. *Hdgfrp2* KO strategy and characterization of MEF cells. (**A**) Shown are salient features of the pGT2lfx gene trap vector, the endogenous and mutated *Hdgfrp2* gene, the fused message that is produced in the trapped cells and the HRP2 PWWP domain fusion protein, as well as the PCR primers that were used to monitor the gene trap allele (AE2511/AE2512 and AE3747/AE3748) and *Hdgfrp2* expression levels (AE3160/AE3161 and AE2553/AE2554). En2 SA, engrail homolog 2 splice acceptor; pA, polyadenylation signal; β-geo, fusion of β-galactosidase and neomycin transferase. (**B**) QRT-PCR analysis of *Hdfgrp2* expression. Exon 1/2 (gray) and exon 5/7 (black) values were normalized to the levels in +/+ WT cells, with each set to 100%. Error bars represent the variation obtained from three replicates using independent mRNA samples. (**C**) Western immunoblot analysis of β-geo and mHRP2 protein expression; β-actin was probed as a loading control. Numbers to the right reflect migration of mass standards in kDa. (**D**) Normalized luciferase values in HIV-Luc-infected +/+, +/g and g/g cell lysates. Error bars show the variation from duplicate infection, luciferase and Bradford assays (RLU, relative light unit). Similar results were observed in three independent experiments.

by the manufacturer (Life Technologies). Following 12 min at 95°C, reactions were cycled 30 times at 95°C for 30 s, 58°C for 30 s, and 72°C for 1 min. Reaction products fractionated by electrophoresis through agarose gels were detected by staining with ethidium bromide.

RNA extraction and quantitative (q) RT-PCR

The concentration of RNA extracted from MEF cells using the RNeasy Mini Kit (Qiagen) was determined by spectrophotometry. Duplicate qRT-PCR mixtures contained 0.5 μM primers, 1×Quantitect SYBR green master mix, 0.3 μl QuantiTect RT mix (QuantiTect Sybr Green RT-PCR kit), and 25 ng of RNA. LEDGF/p75 expression was monitored using primers AE2624/AE2625, which target *Psip1* exons 2/3 (15). Primers AE3160/AE3161 target *Hdgfrp2* exon 1/2 and downstream exon 5/7 sequences were amplified using primers AE2553/2554 (Figure 1A). Data were normalized to *Ppia*, which encodes cyclophilin A, using primers AE3664/AE3665. Reactions were incubated at 50°C for 30 min and then 95°C for 15 min, followed by 40 cycles of 15 s at 94°C, 15 s at 55°C, and 30 s at 72°C. Amplification specificity was confirmed by melting curve analysis from 55°C to 90°C.

Viruses and infection assays

Single-round virus vectors that carry and express the luciferase reporter gene were generated by co-transfecting HEK293T cells with the vesicular stomatitis virus (VSV) G expression vector pCG-VSV-G and either pNLX.Luc.R- (HIV-Luc) or pFB-Luc (MLV-Luc) (15). HIV-Luc was titered using an exogenous reverse transcriptase (RT) assay. MEFs (4×10^4) seeded in 12-well plates were infected in duplicate with 10^6 RT-cpm for 8 h, which corresponds to an approximate multiplicity of infection of 0.06 (32). Cells harvested at 48 h from the start of infection were processed for luciferase activity, and results are expressed as relative light units (RLUs) per total μg protein in cell extracts as determined by Bradford assay (15). For back complementation assays, E9 double-KO cells (5×10^6) were transfected with 10 μg DNA using MEF Nucleofector solution 1 (Amaxa) according to the manufacturers instructions. Transfected cells were plated in 10 cm dishes for 24 h prior to fluorescence activated cell sorting to select green fluorescent protein (GFP)-positive transfectants. After sorting, cells (2×10^4) were seeded in wells of a 24-well plate prior to HIV-Luc (10^6 RT-cpm) infection in duplicate. RLU/μg values from cells transfected with empty vector pIRES2-eGFP were subtracted from experimental samples.

HIV-1 reverse transcription and integration

MEFs (3×10^5) seeded in 10 cm plates were infected with 2×10^7 RT-cpm of DNase-treated HIV-Luc for 2 h. Cells were collected by typsinization, 20% were lysed for genomic DNA extraction, and remaining cells were plated in 4 wells of a 6-well plate for subsequent harvest at 8, 24 and 48 h from the start of infection. Three different sets of PCR primers and probes were used to monitor reverse transcription and integration. Primers AE2963/AE4422 and probe AE2965 detect HIV-1 DNA late reverse transcription (LRT) products whereas sequences

specific for 2-long terminal repeat (LTR) containing circles were amplified using primers AE4450/AE4451 and probe AE4452 (15,33–35). Duplicate reactions that consisted of 20–30 ng of DNA, 0.2 μM primers, 0.1 μM probe, and 1 × QuantiTect Probe PCR Master Mix were incubated at 50°C for 2 min and then 95°C for 15 min, followed by 40 cycles of 15 s at 94°C, 30 s at 58°C and 30 s at 72°C. Serial dilutions of plasmids pNLX.luc.R- and pUC19.2LTR in uninfected cell genomic DNA were used to generate LRT and 2-LTR circle standard curves, respectively (35). Integration efficiency was quantitated by nested BBL-PCR essentially as previously described (15). Duplicate first-round PCRs amplified sequences between integrated virus and flanking genomic B1, B2 or LINE-1 using primers AE3014, AE2604, AE2605, AE2606, AE2607, AE2608 and AE2609 (4,15). The amplification program was 5 min at 94°C, followed by 18 cycles of 30 s at 94°C, 30 s at 60°C and 5 min at 70°C; reactions were terminated following a final 10 min extension at 72°C. DNA (1–2 μl) was amplified in second round using primers AE3013/AE990 and probe AE995 (4,15); the qPCR recipe and program was the same as above. The BBL-PCR standard curve was made by step-wise dilution of DNA from HIV-Luc-infected WT ++/+g cells in uninfected cell DNA. To account for plasmid DNA carryover from transfected cell supernatants in the infections, parallel samples were prepared in the presence of 100 μM azidothymidine, and resulting qPCR values were subtracted from experimental samples.

For monitoring total viral DNA load over 2 weeks, MEFs (2×10^5) seeded in 6-well plates wells were infected with 5×10^6 RT-cpm of HIV-Luc.

Western immunoblot

Whole cell lysates were used to monitor HRP2 protein whereas LEDGF/p75 was detected in lysates of isolated nuclei as described (15). The concentration of protein in extracts was determined by using the Bradford assay, and 2 μg of nuclear material and 10 μg of whole cell extract was fractionated by electrophoresis on sodium dodecyl sulfate polyacrylamide gels. LEDGF/p75 was detected using a 1:10 000 dilution of rabbit antibody A300-848 A-1 (Bethyl Laboratories). Affinity purified rabbit antibody generated against a peptide from the C-terminal 20 residues of mHRP2 (CQDHERTRLASESANDDNEDS) (Bethyl Laboratories) was used at 1:5000. Ectopic expression of LEDGF/p75-HA and HRP2-HA proteins were detected using horseradish peroxidase-conjugated anti-HA antibody (Roche) at 1:5000. Secondary antibody (1:10 000 dilution of conjugated goat anti-rabbit; Dako North America) was followed by detection with the ECL prime reagent (Amersham).

PIC integration activity

PICs were isolated from cytoplasmic and nuclear extracts of E9 cells 7 h after acute infection, and *in vitro* integration activity was measured by nested PCR as described (4,15,30). Two controls were used to define assay background. First, parallel mock integration reactions were run in the absence of the plasmid target DNA. The first-round PCR amplifies covalently joined HIV-plasmid sequences, so, in the second control reaction plasmid-specific primers were omitted from parallel first-round reactions to control for carry over of HIV-1 sequences into the HIV-specific second-round qPCR (4). Both control values were subtracted from experimental samples. Resulting levels of IN-mediated DNA-strand transfer were normalized to the total level of HIV-1 DNA in each extract.

Integration site determination

Genomic DNA isolated from MEF cells 2 d after infection was purified as indicated above. The methods used to shear and amplify the DNA for sequencing by Illumina were based on those described in reference (36). In brief, DNA (5 μg) was sheared into ~300–500 bp fragments using adaptive focused acoustics (Covaris), and purified using AMPure XP magnetic beads (Beckman Coulter). The fragments were end-repaired, dA-tailed and ligated to a double-stranded linker as instructed by the manufacturer. Both first- and second-round amplifications were multiplexed in separate tubes to increase the diversity of the integration site libraries. DNAs were sequenced on an Illumina GA2x machine, and results were parsed to remove duplicate insertion sites. The integration sites were annotated for various genomic features such as genes, transcriptional activity, promoter regions and CpG islands as described previously (37).

Antiviral activity assay

BI-D, a potent ALLINI that binds IN at the LEDGF/p75 binding site (28), was synthesized as described in Supplementary Methods. E9 MEF cells (5×10^3) seeded in wells of a 96-well plate were infected in quadruplicate with HIV-Luc (5×10^5 RT-cpm) in the presence of serial dilutions of BI-D or dimethyl sulfoxide solvent control to determine half-maximal inhibitory concentration (IC_{50}) values of the drug. Luciferase activity was determined 2 d post-infection.

Ethics statement

Mice were maintained at the Beth Israel Deaconess Medical Center (BIDMC, Boston, USA) under guidelines set forth by the USDA and US National Institutes of Health Office of Lab Animal Welfare. The BIDMC IACUC approved animal protocol number 038-2012 'Breeding LEDGF and HRP2 knockout mice'.

RESULTS

Generation of *Hdgfrp2* KO mice and cells

The ability of LEDGF/p75 to support HIV-1 integration depends critically on both the PWWP domain and IBD (13,15,22), and both of these domains are conserved in HRP2 (23). The amino acid sequence of mouse HRP2 (mHRP2) is 81% identical to the human ortholog and 90% similar when evolutionarily conservative substitutions are considered. The amino acid sequences of the PWWP domains of the human and mouse proteins are

identical, whereas the sequences of their IBDs are 92.7% identical and 96.3% similar considering conservative substitutions (38) (Supplementary Figure S1A). To assess the utility of murine cells for studies of HIV-1 infectivity, an *in vitro* GST pull-down assay was used to determine the relative binding affinities of mouse and hHRP2 IBDs for HIV-1 IN protein. As expected, the negative control GST protein failed to pull-down a detectable level of IN (Supplementary Figure S1B, lane 7) (23,30). Also as anticipated, the GST-HRP2 IBD proteins pulled-down less IN than the GST-LEDGF/p75 control protein (18,23,24) (Supplementary Figure S1B, lanes 8–10). Because both HRP2 IBDs recovered similar levels of HIV-1 IN (Supplementary Figure S1C), the minor amino acid differences in the IBDs between the human and mouse proteins does not have a significant impact on IN-binding affinity under these conditions.

Hdgfrp2 KO mice were generated from embryonic stem (ES) cells obtained at BayGenomics, who use a gene trap vector to disrupt the function of endogenous genes (39). The pGT2lfx vector, which carries a reporter gene for the β-galactosidase-neomycin phosphotransferase (β-geo) fusion protein downstream from a strong splice acceptor site and upstream from a polyadenylation signal, was integrated between exons 3 and 4 of *Hdgfrp2*, which would lead to the expression of a 1423 residue PWWP-β-geo fusion protein (Figure 1A). Chimeric mice generated following ES cell implantation were bred with C57BL/6 animals, and heterozygous +/g (g for gene trap) animals were interbred to generate WT +/+, heterozygous +/g and homozygous g/g animals. The g/g animals survive until adulthood and are fertile; a detailed characterization of *Hdgfrp2* and *Hdgfrp2*/*Psip1* double-KO animals will be presented elsewhere.

Deletion of part or all of an endogenous gene yields genetically null phenotypes whereas gene trap KOs carry a targeted insertion. Thus, the impact of the KO relies on the efficiency of the trap (40,41). MEF cells isolated from 13.5-day post-cotium embryos were adapted for long-term culture by transformation with SV40 large T antigen as described (31). To assess the relative strength of the *Hdgfrp2* trap, mRNA derived from +/+, +/g and g/g cells was monitored by qRT-PCR using primers that amplify sequences upstream (exons 1/2) and downstream (exons 5/7) of the insertion (Figure 1A). The levels of upstream exonic sequences in heterozygous +/g and homozygous g/g cells were about 57% and 33% of the level of WT +/+ cells. The level of downstream exon 5/7 sequences present in the heterozygous cells was about 44% of the WT level whereas these sequences varied from barely detectable to ~5% of the WT in g/g cells (Figure 1B). *Hdgfrp2* expression was also analysed by RNAseq, which yielded strikingly similar results: RNA sequences corresponding to the upstream exons were readily detected, but only very low levels of RNA corresponding to the downstream exons were present in g/g cells (data not shown). The predicted 161 kDa PWWP-β-geo fusion protein was readily detected by western blotting +/g and g/g cell extracts. As expected from the qRT-PCR analysis, g/g cells did not contain a detectable level of mHRP2 protein (Figure 1C).

Hdgfrp2 KO cells support normal levels of HIV-1 infection

To assess the role of HRP2 protein in HIV-1 infection, MEF cells were infected with a single-round HIV-1 vector that carries and expresses the gene for firefly luciferase (HIV-Luc). Two days post-infection, levels of luciferase activity were normalized to the total protein content in the cell extracts. Each cell type supported similar levels of luciferase activity (Figure 1D). Therefore, HRP2 does not play an essential role in HIV-1 infection under these experimental conditions.

Generation and characterization of MEFs from *Hdgfrp2*/*Psip1* double-KO animals

Our findings with *Hdgfrp2* g/g cells are consistent with previous reports that failed to detect a role for HRP2 in HIV-1 infection using RNAi (13,18,27). We next sought to determine if removing LEDGF/p75 might reveal a phenotype for the HRP2 KO. Because *Hdgfrp2*-disrupted cells support efficient infection (Figure 1D) and adult g/g animals are fertile, heterozygous +−/+g animals were interbred with +−/gg animals. The latter mice, which are heterozygous for *Psip1* KO but homozygous for the *Hdgfrp2* gene trap, were used to increase the odds of obtaining the desired WT and single- and double-KO embryos from the same litter. All of the mice that resulted from this breeding scheme carried at least one gene trap allele: WT, ++/+g; HRP2 KO, ++/gg; LEDGF/p75 KO, −−/+g; double KO, −−/gg. The term 'WT', in the context of the double KO, accordingly refers to heterozygous +/g animals. Pregnant females were dissected at day 13.5 post-cotium until two complete sets of matched embryos were obtained (denoted E9 and E13; Supplementary Figure S2). Expression profiling confirmed the different KO phenotypes among the cell types from each set of embryos. The growth rates of the single- and double-KO cells from each set were similar to the matched WT cells (Supplementary Figure S2 and data not shown).

Both sets of cells were infected with HIV-Luc, and luciferase activities in cell extracts were determined as above. As expected from Figure 1D, each *Hdgfrp2* KO cell line supported a similar level of HIV-Luc infection as the matched WT control (Figure 2A and B). The *Psip1* KO cells from the E13 set supported about 21% of the level of infection observed with the matched ++/+g cells whereas the E9 *Psip1* KO supported about 11% of the matched control. In both cases, the addition of the *Hdgfrp2* KO reduced infectivity about 2-fold, with the E13 and E9 double-KO cells supporting about 11.3% and 5.9% of the level of the matched infection with the respective WT control cells (Figure 2A and B). In both cases, the difference between *Psip1* KO and double-KO cells was statistically significant.

Cells were also challenged with two control viruses. Infections with N/N-Luc, which carries two inactivating mutations (D64N/D116N) in the IN active site, results in low levels of luciferase activity despite the absence of IN activity due to inefficient cell-mediated DNA recombination and/or transcription from unintegrated DNA templates (42,43). The various cells from the E9 set each

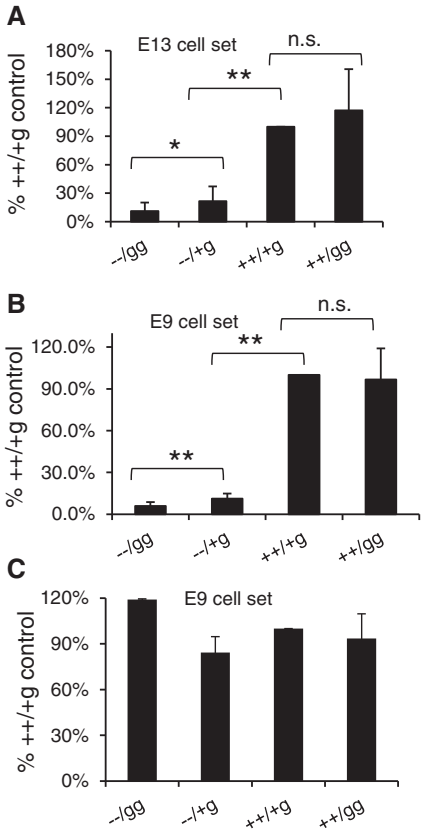

Figure 2. HIV-1 but not MLV is defective for infection of *Hdgfrp2*/*Psip1* double-KO cells. (**A**) Normalized levels of HIV-Luc infection of littermate control sets of E13 cells. Plotted are averages and standard deviations from pooled independent sets of experiments ($n = 6$), with the level of WT ++/+g RLU/μg set to 100%. (**B**) Similar to panel A, except the E9 set of cells was analysed in $n = 5$ experiments. (**C**) MLV-Luc titers on the indicated E9 cell lines for $n = 2$ independent experiments. n.s., not significant; $^{*}P < 0.05$; $^{**}P < 0.01$ as determined by one-tailed Student's *t*-test.

supported similar levels of N/N-Luc activity, which varied from about 0.09% to 0.14% of the level of HIV-Luc expression in WT ++/+g cells. Based on these results, we conclude that the different levels of HIV-Luc infection across the various cell types depended on functional IN activity and that the double-KO cells support a residual level of HIV-Luc integration that is, based on comparative HIV-Luc and N/N-Luc titers, minimally 40-fold over background. MLV-Luc was used as a positive control virus. MLV IN does not bind LEDGF/p75 (44,45) and as expected, MLV-Luc infected the different cell types at a similar efficiency (Figure 2C).

HRP2 KO causes an integration defect in LEDGF/p75 KO cells

Psip1 KO cells support normal levels of HIV-1 reverse transcription but reduced levels of virus integration (15,17,18). To investigate the cause of the additional defect in infection seen in *Hdgfrp2*/*Psip1* double-KO cells, DNA synthesis, nuclear migration and integration were monitored by qPCR using three sets of primers/probes. Viral R and *gag*-specific primers yield products that reflect the total viral DNA synthesized, whereas U5 and U3 primers amplify 2-LTR circles that form in the nucleus through the action of non-homologous end-joining machinery (34). Integration in human cells is often measured using PCR anchored through the repetitive *Alu* element. Because *Alu* is a primate-specific repeat, our mouse cell integration assay uses the B1, B2 and LINE-1 repeat sequences (BBL-PCR) (15). IN inhibitors or inactivating IN mutations quantitatively block integration and increase the proportion of linear viral DNA molecules available for circularization in the nucleus. An increase in the amount of 2-LTR circles is therefore indicative of failed integration (35,46).

The level of viral DNA synthesis, which peaked at 8 h post-infection and diminished thereafter, was similar across the 4 different cell types (Figure 3A). As expected, the level of HIV-1 integration in WT and *Hdgfrp2* KO cells was similar at 2 days post-infection (Figure 3B). Also as expected, integration in *Psip1* KO cells was reduced compared with the WT cells, by about 2.5-fold in these assays. Because integration in double-KO cells was further reduced (to about 10% of the level in WT cells), we conclude that a lower level of integration underlies the reduced level of infection by the HIV-Luc vector in the double KO as compared with *Psip1* KO cells. This interpretation is supported by two additional observations. Consistent with an integration defect, the level of 2-LTR circles in *Psip1* KO cells was about 2.5-fold higher than in WT cells at 24 h post-infection (Figure 3C) (13–15). A further increase in the level of 2-LTR circles, which amounted to approximately a 5-fold increase over that observed in WT cells, was seen in the *Psip1*/*Hdgfrp2* double-KO cells, which is consistent with the decreased level of integration. Secondly, total viral load was profiled over a 2-week time course. Because unintegrated viral DNA is not replicated, it is diluted in cultures of dividing cells (34). Experiments that use HIV-based vectors to knockdown host factors have taken advantage of the decay in unintegrated viral DNA over time to gauge the relative integration levels in subsequent viral challenges (13,17). The total level of HIV-1 DNA in WT and *Hdgfrp2* KO cells was similar at 2 weeks post-infection. However, the levels in *Psip1* and *Psip1*/*Hdgfrp2* KO cells were ~25% and 12% of the level in WT cells, respectively (Figure 3D). Thus, the efficiency of viral DNA integration correlates with relative level of HIV-1 infection in the four cell types (Figures 2 and 3).

The integration defect in *Psip1*/*Hdgfrp2* KO cells correlates with PIC activity

We previously determined that HIV-1 PICs made in *Psip1* KO cells are fully competent to integrate the viral reverse transcript *in vitro* (15). To determine if the remaining HRP2 in these cells might influence PIC function, cytoplasmic and nuclear material extracted from cells 7 h from the start of infection were incubated with plasmid target DNA in the presence of Mg^{2+} ions. Purified DNAs were examined by nested qPCR to detect the formation of covalent HIV-plasmid DNA junctions, and these values

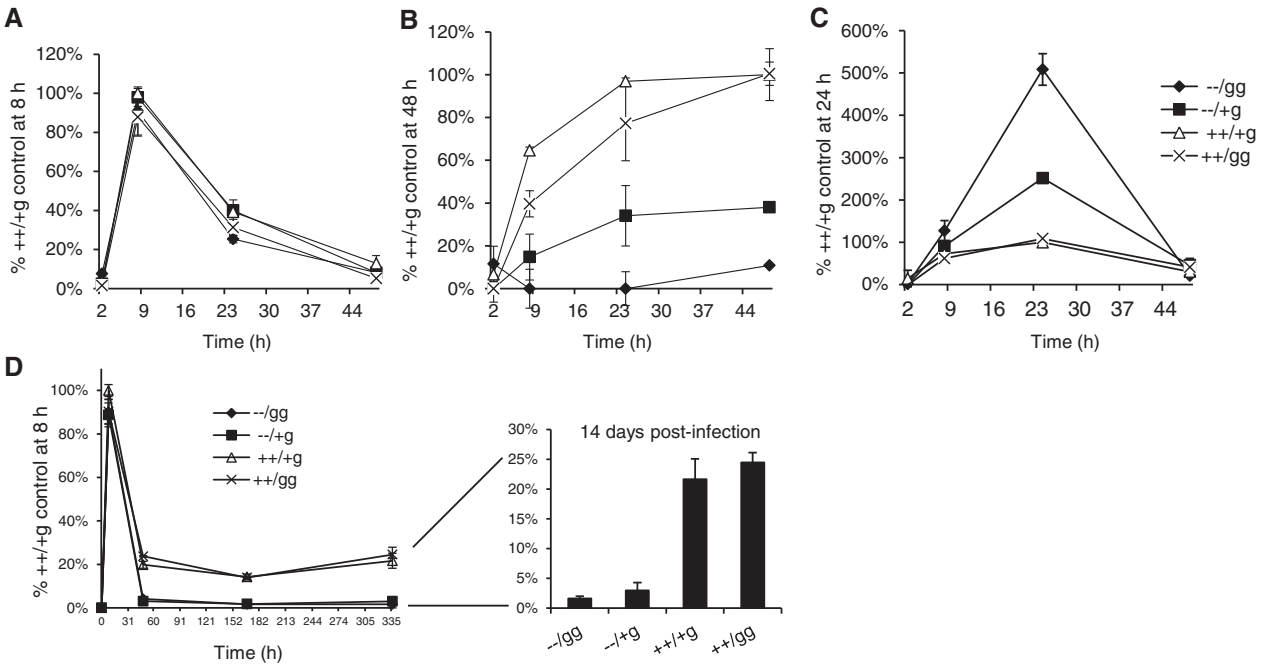

Figure 3. HIV-1 reverse transcription and integration. (**A**) Levels of qPCR products were determined at the indicated time points using E9 WT (open triangles), *Hdgfrp2* KO (cross marks), *Psip1* KO (filled boxes) and double-KO (filled diamonds) cells. The results were normalized to the WT cell 8 h time-point, which was set at 100%. (**B**) BBL-PCR values for the extracts described in panel (A). Results were normalized to the WT sample at 48 h, which was set to 100%. (**C**) 2-LTR circle levels for panel (A) samples, normalized to the WT cell value at 24 h post-infection (set at 100%). (**D**) Total HIV-1 DNA load over a 2-week time course. The panel at the right shows the 2-week values. Error bars are the variation obtained from duplicate sets of PCR assays. Results are representative of those obtained in two (panel (D)) or three (panels (A)–(C)) independent experiments.

were normalized to the total level of HIV-Luc DNA in the extracts. As expected, PICs extracted from *Psip1* KO cells showed levels of integration activity similar to PICs extracted from WT and *Hdgfrp2* KO cells (Figure 4). PICs extracted from double-KO cells supported about half this level of activity, linking the drop in chromosomal integration in double-KO cells to a reduction in the strand transfer activity of PIC-associated IN.

Differential effects of *Psip1* and *Hdgfrp2* KO on integration site distribution

In addition to influencing the overall efficiency of integration, LEDGF/p75 in large part determines the propensity for HIV-1 to integrate within the bodies of active genes (15,17–19). To ask whether HRP2 KO might also contribute to integration targeting, high molecular weight DNA isolated 2 days after infection was sheared, end-repaired, amplified by ligation-mediated PCR and sequenced by Illumina to determine the genomic sites of HIV-1 DNA integration. The integration datasets, which were initially parsed to remove duplicate sequences, were analysed for numerous genomic features including genes, gene density and areas nearby transcription start sites (TSSs) and CpG islands (Table 1; see Figure 5 for corresponding statistical analyses). The data presented here are from the E13 set of MEF cells; similar results were obtained using the E9 cell set (data not shown).

In agreement with prior findings (15,17–19), the LEDGF/p75 KO significantly reduced the frequency of integration within transcription units (from 68.9% to

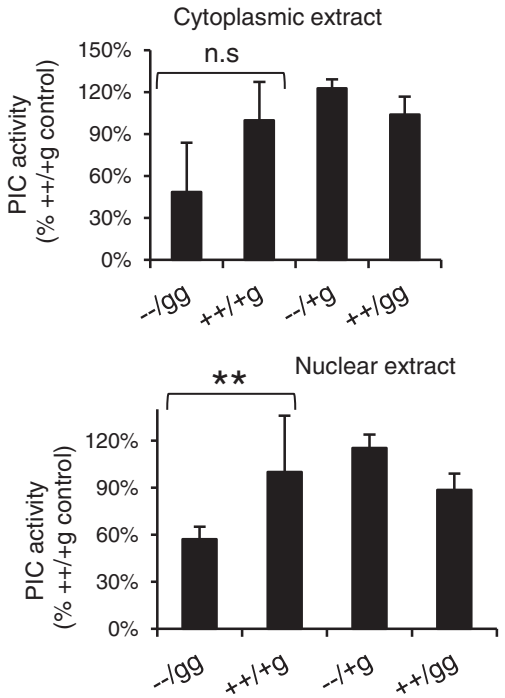

Figure 4. *In vitro* integration activities of PICs. Strand transfer activities, normalized to the levels of HIV-Luc substrate DNA in the extracts, are plotted as percent activities in WT E9 cell extracts. Error bars represent the variation obtained from duplicate sets of PCR assays; results are representative of those observed in two (cytoplasmic PICs) to three (nuclear samples) independent experiments. $^{**}P < 0.01$ as determined by one-tailed Student's *t*-test; the lack of statistical significance in the cytoplasmic samples is in part due to the extent of variation among duplicate PCR samples.

Table 1. Integration site usage among cell type

Annotation	Random	WT MEFs	HRP2 KO	LEDGF KO	Double KO	Double KO + hHRP2	Double KO + hLEDGF
Unique integrations	100 000	381 429	146 243	130 867	80 483	62 657	134 169
Within a gene	33 031 (33.0%)	262 774 (68.9%)	100 453 (68.7%)	56 894 (43.5%)	32 199 (40.0%)	41 194 (65.8%)	87 142 (65.0%)
+/− 1 kB of a TSS	1595 (1.60%)	2104 (0.55%)	747 (0.51%)	4652 (3.55%)	2852 (3.54%)	974 (1.55%)	1023 (0.76%)
+/− 1 kB of a CpG island	728 (0.73%)	1334 (0.35%)	460 (0.31%)	2800 (2.14%)	1667 (2.07%)	767 (1.22%)	634 (0.47%)
Avg. genes per Mb	8.5	14.0	14.2	10.7	10.8	15.0	13.3

Refseq genes from mouse genome build mm9, UCSC Genome Bioinformatics website.

43.5%), with concomitant increases in integrations near TSSs and CpG islands. We also note that integration into gene dense regions was significantly reduced in cells lacking LEDGF/p75. Though this result differs from prior published reports (17,47), it is reproducibly observed in relatively large data sets of integrations in *Psip1* KO cells (Y. Koh *et al.*, submitted for publication). As expected, the LEDGF/p75 KO also significantly altered the ability of HIV-1 to integrate into active genes (Figure 6). With the exception of integration nearby CpG islands, which likely attained a modest significance due to our large datasets ($P = 0.037$), the *Hdgfrp2* KO did not significantly impact the frequencies at which HIV-1 targets mouse genomic features (Table 1; Figures 5 and 6). Compared with the *Psip1* KO alone, adding the *Hdgfrp2* KO significantly reduced the frequency at which HIV-1 integration targeted active genes, although integration into gene dense regions and nearby TSSs and CpG islands was not significantly affected (Table 1; Figures 5 and 6). HRP2 therefore contributes to the targeting of HIV-1 PICs to active genes, a result that is revealed when the dominant IN-binding protein, LEDGF/p75, is absent from the cell.

HIV-1 integration is modestly influenced by the nucleotide sequence at the site of insertion (10,48), a trait that is not significantly altered by *Psip1* KO (15,17,18). The sequences listed in Table 1 were queried to determine if dual depletion of HRP2 and LEDGF/p75 might influence local sequence preference during integration. This analysis revealed that the preferred target DNA integration sequence TDG↓GTWACCHA (↓ indicates the position of plus-strand joining) (10,48) was not affected by the presence or absence of either LEDGF/p75 or HRP2 (Supplementary Figure S3).

Ectopic LEDGF/p75 or HRP2 expression restores HIV-1 titer and integration specificity to double-KO cells

Expressing hLEDGF/p75 in *Psip1* KO MEFs restores HIV-1 infectivity (15). To determine whether HRP2 might also function under these conditions, double-KO cells transfected with vectors that express both the protein of interest and GFP were sorted for GFP expression, plated and challenged with HIV-Luc (15). Two days later, levels of HIV-Luc infectivity (Figure 7) and genomic sites of HIV-1 integration (Table 1) were determined. Expression of hHRP2 or mHRP2 stimulated HIV-Luc infection to about 60% and 34% of the level observed with hLEDGF/p75, respectively (Figure 7). Two different hHRP2 mutants were tested for their ability to rescue HIV-1 integration and infection. In one mutant, the N-terminal PWWP domain was deleted; in the other, the Asp residue that corresponds to Asp366 in the LEDGF/p75 IBD, which makes critical H-bond contacts with the backbone amides of IN (49), was substituted by Asn (D489N). Neither of these mutants increased the level of HIV-Luc infection above the background seen with the empty vector in pIRES2-eGFP transfected cells. We therefore conclude that HRP2 rescue of HIV-1 infection requires both the specific interactions with IN provided by the IBD, and with chromatin provided by the PWWP domain. Accordingly, expression of either hHRP2 or hLEDGF/p75 was able to restore, in large part, the normal profile of integration targeting in the double-KO cells, although the effect of hHRP2 on integration nearby TSSs and CpG islands was somewhat more modest than that of hLEDGF/p75 (Table 1).

Contribution of LEDGF/p75 and HRP2 to the antiviral activity of a potent ALLINI

Different approaches have been used to identify antiviral compounds that engage IN at the LEDGF/p75 binding site. One approach depended on detecting a perturbation of host factor-IN binding (50) whereas a separate effort screened for inhibitors of IN 3′ processing activity (28,51). In addition to blocking the LEDGF/p75-IN interaction, it has recently become clear that these compounds inhibit the assembly of the stable synaptic IN-viral DNA complex and thus affect IN activity in a LEDGFp75-independent manner *in vitro* (51–53). The compounds also remain active in *PSIP1* KO cells, suggesting that their ability to disrupt the HRP2-IN interaction could contribute to their antiviral activity (18). Our novel MEF cell lines presented an excellent opportunity to determine the contribution of LEDGF/p75 and HRP2 to the antiviral activity of ALLINIs. BI-D, a representative of this class of inhibitors (28), was synthesized as described in Supplementary Methods. The IC_{50} of the BI-D inhibitor was determined during the acute phase of HIV-1 infection, at the time LEDGF/p75 and HRP2 are known to function. Approximately 2.4–2.9 μM of BI-D was required to inhibit 50% of HIV-Luc infection of WT and *Hdgfrp2* KO cells, while the IC_{50} decreased dramatically, to 160–200 nM, in *Psip1* and double-KO cells.

		WT	HRP2 KO	LEDGF KO	Double KO	Double KO + hHRP2	Double KO + hLEDGF
Within a gene	random	<0.0001	<0.0001	<0.0001	<0.0001	<0.0001	<0.0001
	WT cells	***0.153***	<0.0001	<0.0001	<0.0001	<0.0001	<0.0001
	LEDGF KO				<0.0001	<0.0001	<0.0001
	Double KO					<0.0001	<0.0001
± 1 kB of a TSS	random	<0.0001	<0.0001	<0.0001	<0.0001	***0.53***	<0.0001
	WT cells	***0.07***	<0.0001	<0.0001	<0.0001	<0.0001	<0.0001
	LEDGF KO				***0.90***	<0.0001	<0.0001
	Double KO					<0.0001	<0.0001
± 1 kB of a CpG island	random	<0.0001	<0.0001	<0.0001	<0.0001	<0.0001	<0.0001
	WT cells	0.037	<0.0001	<0.0001	<0.0001	<0.0001	<0.0001
	LEDGF KO				***0.30***	<0.0001	<0.0001
	Double KO					<0.0001	<0.0001
Average genes/Mb	random	<0.0001	<0.0001	<0.0001	<0.0001	<0.0001	<0.0001
	WT cells	***0.217***	<0.0001	<0.0001	<0.0001	<0.0001	0.019
	LEDGF KO				***0.088***	<0.0001	<0.0001
	Double KO					<0.0001	<0.0001

Figure 5. Statistical analysis of integration site targeting frequencies among cell type. Pairwise comparisons of the indicated Table 1 datasets were analysed using Fisher's exact test to determine statistical significance of HIV-1 integration within genes as well as nearby transcriptional start sites and CpG islands. Integration into gene dense regions of chromosomes, expressed as average number of genes per Mb, was analysed by Mann–Whitney rank sum test. *P*-values > 0.05 are highlighted in bold italics.

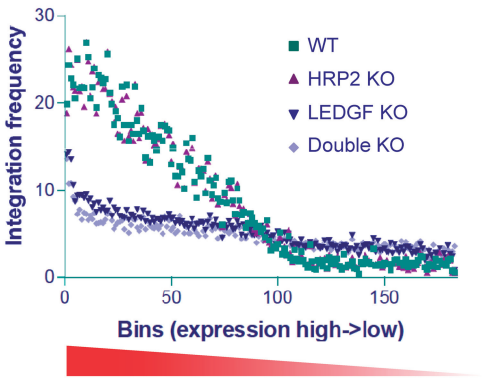

Figure 6. Integration as a function of gene expression. Refseq genes are sorted by expression along the *x*-axis from high to low in bins of 100 genes each. Integration sites within genes in each bin were counted and normalized by the size of the bin and the total number of integration sites (per Mb region/10 000 sites). Paired Wilcoxon matched *t*-test analysis revealed the following statistically relevant ($P < 0.0001$) comparisons: WT versus LEDGF KO; WT versus double KO; LEDGF KO versus HRP2 KO; LEDGF KO versus double KO; HRP2 KO versus double KO; and WT, LEDGF KO, HRP2 KO, double KO versus random. In contrast, the WT and HRP2 KO profiles did not differ significantly from one another ($P = 0.9992$).

In contrast, the IC_{50} value for the IN active site inhibitor raltegravir was similar in each cell type (Table 2).

DISCUSSION

To address the roles of LEDGF/p75 and HRP2 in HIV-1 infection and integration, we developed littermate-matched cell lines knocked out for each of these factors, as well as double-KO cell lines that lack both factors. While targeted deletion was used to KO *Psip1* (15), *Hdgfrp2* was disrupted by insertion of the pGT2lfx gene trap vector. The position of vector integration can influence the efficiency of a trap (40), and expression profiling by both qRT-PCR (Figure 1B and Supplementary Figure S2B) and RNAseq (data not shown) indicated that downstream exonic sequences could be expressed in homozygous g/g cells at relatively low levels (up to 5% of the level observed in WT cells). Although we were unable to detect a corresponding level mHPR2 protein by western blotting, we cannot dismiss the possibility that a low level of functional mHRP2 persists in g/g or *Psip1*/*Hdgfrp2* KO cells. Gene trap insertion was previously used to disrupt *Psip1* expression and, similar to the results reported here, a low

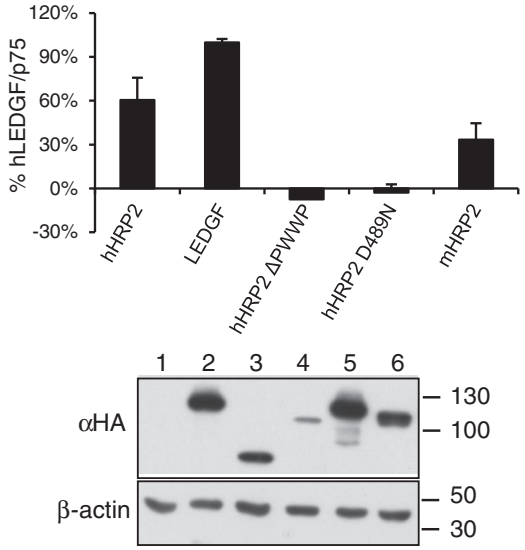

Figure 7. Ectopic LEDGF/p75 and HRP2 expression each restore HIV-1 infection to double-KO cells. Shown are RLU/μg values normalized to the level of infection of LEDGF/p75-expressing cells, which was set to 100%. Error bars are the variation obtained from duplicate conditions (infection, luciferase and Bradford assays). Lower panels, immunoblot of hHRP2 (lane 2), hLEDGF/p75 (lane 3), hHRP2ΔPWWP (lane 4), hHRP2/D489N (lane 5) and mHRP2 (lane 6) expressing cells; the extract loaded in lane 1 came from cells transfected with the empty vector. Results are representative of those observed in two independent experiments.

Table 2. Raltegravir and BI-D IC_{50} values

	WT ++/+g	HRP2 KO ++/gg	LEDGF KO −−/+g	Double KO −−/gg
Raltegravir IC_{50} (nM)	4.0 ± 1.5	3.2 ± 1.2	5.6 ± 1.0	4.8 ± 2.9
BI-D IC_{50} (μM)	2.9 ± 1.5	2.4 ± 1.0	0.16 ± 0.09	0.20 ± 0.09

Mean ± standard deviation for $n = 4$ independent experiments.
BI-D IC_{50} value statistics (Student's *t*-test): WT versus HRP2 KO, n.s.; LEDGF KO versus WT, $P < 0.05$; double KO versus LEDGF KO, n.s.; WT and HRP2 KO versus LEDGF KO and double KO, $P < 0.001$.

level of *Psip1* message was read through that trap (16). Because *Psip1* KO cells produced by gene trap insertion and chromosomal deletion behave indistinguishably in assays for HIV-1 infection and integration (15,17), we infer that if there is a low level of mHRP2 protein in homozygous g/g cells, it is unlikely to have a significant impact on the efficiency or specificity of HIV-1 integration.

Although mouse cells present numerous blocks to HIV-1 replication (54), they are efficiently transduced by pseudovirions, a trait that we and others have used to study the roles of host factors in the early stages of HIV-1 infection (15,17,31,55–57). The PWWP domains of hHRP2 and mHRP2 are identical, and the minor amino acid variation between these IBDs does not have an obvious impact on HIV-1 IN-binding affinity (Supplementary Figure S1). Hence, mouse cells afford a convenient model for studying the roles of both LEDGF/p75 and HRP2 in HIV-1 integration. By extension, these cells are useful reagents to investigate the roles of LEDGF/p75-IN and HRP2-IN interactions in the antiviral activities of ALLINIs that target the host factor-binding site at the IN CCD dimer interface.

HRP2 and HIV-1 integration

HIV-1 infection and integration site distribution were largely unaffected by the HRP2 KO. It is important to appreciate the fact that early attempts to knockdown LEDGF/p75 expression using RNAi failed to reveal a role for the protein in HIV-1 infection despite achieving potent reductions in the steady-state level of the host factor (27,44). These conditions nevertheless altered the specificity of integration (19), showing that the minute amounts of LEDGF/p75 that are sufficient to support normal levels of HIV-1 infection nevertheless fail to sustain the specificity of PIC/integration targeting. Subsequently, more stringent knockdowns and LEDGF/p75 KOs revealed the central role of this host factor-in mediating both the efficiency and specificity of HIV-1 integration (13,15,17,18). The fact that the *Hdgfrp2* KO does not affect HIV-1 targeting of genomic features argues against a significant role for this secondary IN-binding protein in determining the distribution of HIV-1 integration in cells that express LEDGF/p75. This result clarifies the dominant role of LEDGF/p75 as the key IN-binding integration co-factor during the early phase of HIV-1 infection. A significant subsidiary role for HRP2 in HIV-1 integration was revealed by comparing the behavior of the virus in cells knocked out for LEDGF/p75 to cells depleted for both host factors. These data revealed that, under the right conditions, HRP2 could influence HIV-1 PIC activity, which correlated with an ~2-fold reduction in chromosomal DNA integration and loss of targeting to active genes (Figures 5 and 6; Table 1). Although the mechanistic basis for the role of the host factors in PIC function is unclear, models based on the stimulation of IN activity and/or target DNA binding can be considered. LEDGF/p75 and HRP2 each stimulate the DNA-strand transfer activity of HIV-1 IN *in vitro* (23), suggesting that factor-mediated tetramerization of the enzyme (58,59) might play an important role in PIC function. LEDGF/p75 binds DNA non-specifically (21) and although we have not assessed HRP2 DNA-binding activity, the protein harbors sequences similar to the AT-hook DNA-binding motifs in LEDGF/p75 (23), suggesting that it might also engage DNA non-specifically. Additional work with LEDGF/p75 and HRP2 mutant proteins that disrupt DNA and/or IN binding is necessary to further investigate these possibilities. Because double-KO cells support integration at levels significantly above background, we conclude that IN and/or other host factors can contribute to gene targeting during HIV-1 infection in the absence of both HRP2 and LEDGF/p75 (Table 1 and Figure 6).

LEDGF/p75 functions as a bimodal tether during integration: elements in the N-terminal portion of the protein bind to chromatin whereas the downstream IBD binds IN. The viral side of the equation is well understood: co-crystal structures have revealed intimate contacts between the IBD and the CCD dimer interface and α1 of the N-terminal domain of IN (49,60), results that have been confirmed by numerous biochemical and genetic experiments (13,15,38,60). The binding of HRP2 to IN is likely weaker than the corresponding interaction with LEDGF/p75 because of two conservative substitutions at critical IBD contact residues: LEDGF/p75 residues Ile365 and Phe406 are replaced by Val1488 and Tyr529, respectively, in HRP2 (38). The cellular side of the bimodal tether is less well understood. Both LEDGF/p75 and HRP2 are nuclear proteins, but only LEDGF/p75 behaves as a constitutive component of chromatin (24). Nevertheless, HRP2 can direct HIV-1 DNA integration to active genes in the absence of LEDGF/p75 (Figure 6 and Table 1), and it functions efficiently as a co-factor for HIV-1 infection and integration when it is ectopically expressed in double-KO cells. As expected, this rescue of infectivity depends on the N-terminal PWWP domain of HRP2 (Figure 7). These results suggest that HRP2 can interact with chromatin when LEDGF/p75 is depleted from cells. A more detailed understanding of the roles of LEDGF/p75 and HRP2 in HIV-1 integration will come from deciphering the mechanism(s) of the interactions of these PWWP domains with chromatin. It will also be instructive to test whether HRP2 plays a role in physiologically relevant targets of HIV-1 infection, such as monocyte-derived macrophages, that express relatively low levels of LEDGF/p75 protein (17).

Mechanism of action of ALLINIs

Several groups have described similar 2-(quinolin-3-yl)-acetic acid derivatives that inhibit LEDGF/p75-IN binding *in vitro* and integration during the acute phase of HIV-1 infection (50–53). Initially dubbed LEDGINs (LEDGF/p75-IN inhibitors), it has recently become apparent that these compounds inhibit the assembly of IN on viral DNA (51–53), a step that in all likelihood precedes the binding of LEDGF/p75 to IN during HIV-1 infection (61,62). Accordingly, the drugs inhibit IN catalytic function *in vitro* in a LEDGF/p75 independent manner (51–53). We therefore refer to these compounds as ALLINIs or 'allosteric IN inhibitors' to emphasize their host factor-independent mode of action. ALLINIs nevertheless reveal steep dose response curves in antiviral activity assays, indicating inhibition of a functionally multivalent target (51,63). Based on the available *in vitro* data, potential ALLINI targets during HIV-1 infection include assembly of the stable synaptic IN-viral DNA complex and the interaction of the assembled PIC with LEDGF/p75 (51–53). LEDGINs were recently shown to retain activity in *PSIP1* KO cells, suggesting that inhibiting the interaction of HRP2 with IN might be an important target under these conditions (18). We show here that this is unlikely to be the case. The antiviral activity (IC_{50}) of the ALLINI inhibitor BI-D increased significantly, from about 2.9 μM in WT cells to 0.16 μM in *Psip1* KO cells, a result that was not significantly altered by *Hdgfrp2* disruption (Table 2). Our results suggest that LEDGF/p75 competes with the inhibitors for binding at the IN CCD interface during infection, and that HRP2 is less able to compete with the inhibitor because it binds to IN more weakly than LEDGF/p75. If the interactions with IN were the important antiviral targets of the ALLINI inhibitor, we would have expected the IC_{50} to increase in the absence of the key interacting factors, which is not the case.

We and others have observed that HIV-1 produced in the presence of ALLINIs is non-infectious (K. A. Jurado, unpublished observation) (53). The IC_{50} of BI-D in an assay which measures the spread of HIV-1_{NL4-3} in human T cells (51) is ~100 nM (unpublished observations). Because the LEDGF/p75-IN interaction is not thought to play a post-integration role in HIV-1 replication (64), our data indicate that ALLINIs act primarily by engaging IN during virus production to inhibit the subsequent round of stable synaptic IN-viral DNA complex assembly. The strength of the inhibitor is accordingly increased during the early stage of HIV-1 replication when LEDGF/p75 is removed from the system (Table 2), implying that LEDGF/p75 normally engages the PIC soon after IN assembles on the viral DNA (44,65). Our single- and double-KO cells should continue to be valuable agents to investigate LEDGF/p75 function during HIV-1 infection and the multimode mechanism of action of clinically relevant ALLINIs.

SUPPLEMENTARY DATA

Supplementary Data are available at NAR Online: Supplementary Table 1, Supplementary Figures 1–3, Supplementary Methods and Supplementary References [66–70].

ACKNOWLEDGEMENTS

Due to the development of single- and double-KO animals, the scope of this project spanned many years; N. Vandegraaff and J.E. Daigle are accordingly thanked for their contributions to the early phase of the project.

FUNDING

US National Institutes of Health (NIH) [AI039394 to A.E., AI081581 to M.K., AI097044 to J.R.F.]; National Cancer Institute's Intramural Center for Cancer Research, which supports the HIV Drug Resistance Program [to S.H.H.]; UK Medical Research Council [G1000917 to P.C.]. Funding for open access charge: US NIH [AI039394].

Conflict of interest statement. None declared.

REFERENCES

1. Fujiwara,T. and Mizuuchi,K. (1988) Retroviral DNA integration: structure of an integration intermediate. *Cell*, **54**, 497–504.
2. Brown,P.O., Bowerman,B., Varmus,H.E. and Bishop,J.M. (1989) Retroviral integration: structure of the initial covalent product and its precursor, and a role for the viral IN protein. *Proc. Natl Acad. Sci. USA*, **86**, 2525–2529.
3. Farnet,C.M. and Haseltine,W.A. (1990) Integration of human immunodeficiency virus type 1 DNA in vitro. *Proc. Natl Acad. Sci. USA*, **87**, 4164–4168.
4. Engelman,A., Oztop,I., Vandegraaff,N. and Raghavendra,N.K. (2009) Quantitative analysis of HIV-1 preintegration complexes. *Methods*, **47**, 283–290.
5. Bushman,F., Lewinski,M., Ciuffi,A., Barr,S., Leipzig,J., Hannenhalli,S. and Hoffmann,C. (2005) Genome-wide analysis of retroviral DNA integration. *Nat. Rev. Microbiol.*, **3**, 848–858.
6. Schroder,A.R.W., Shinn,P., Chen,H., Berry,C., Ecker,J.R. and Bushman,F. (2002) HIV-1 integration in the human genome favors active genes and local hotspots. *Cell*, **110**, 521–529.
7. Wu,X., Li,Y., Crise,B. and Burgess,S.M. (2003) Transcription start regions in the human genome are favored targets for MLV integration. *Science*, **300**, 1749–1751.
8. Mitchell,R.S., Beitzel,B.F., Schroder,A.R.W., Shinn,P., Chen,H., Berry,C.C., Ecker,J.R. and Bushman,F.D. (2004) Retroviral DNA integration: ASLV, HIV, and MLV show distinct target site preferences. *PLoS Biol.*, **2**, e234.
9. Narezkina,A., Taganov,K.D., Litwin,S., Stoyanova,R., Hayashi,J., Seeger,C., Skalka,A.M. and Katz,R.A. (2004) Genome-wide analyses of avian sarcoma virus integration sites. *J. Virol.*, **78**, 11656–11663.
10. Wu,X., Li,Y., Crise,B., Burgess,S.M. and Munroe,D.J. (2005) Weak palindromic consensus sequences are a common feature found at the integration target sites of many retroviruses. *J. Virol.*, **79**, 5211–5214.
11. Engelman,A. and Cherepanov,P. (2008) The lentiviral integrase binding protein LEDGF/p75 and HIV-1 replication. *PLoS Pathog.*, **4**, e1000046.
12. Poeschla,E.M. (2008) Integrase, LEDGF/p75 and HIV replication. *Cell Mol. Life Sci.*, **65**, 1403–1424.
13. Llano,M., Saenz,D.T., Meehan,A., Wongthida,P., Peretz,M., Walker,W.H., Teo,W. and Poeschla,E.M. (2006) An essential role for LEDGF/p75 in HIV integration. *Science*, **314**, 461–464.
14. Vandekerckhove,L., Christ,F., Van Maele,B., De Rijck,J., Gijsbers,R., Van den Haute,C., Witvrouw,M. and Debyser,Z. (2006) Transient and stable knockdown of the integrase cofactor LEDGF/p75 reveals its role in the replication cycle of human immunodeficiency virus. *J. Virol.*, **80**, 1886–1896.
15. Shun,M.C., Raghavendra,N.K., Vandegraaff,N., Daigle,J.E., Hughes,S., Kellam,P., Cherepanov,P. and Engelman,A. (2007) LEDGF/p75 functions downstream from preintegration complex formation to effect gene-specific HIV-1 integration. *Genes Dev.*, **21**, 1767–1778.
16. Sutherland,H.G., Newton,K., Brownstein,D.G., Holmes,M.C., Kress,C., Semple,C.A. and Bickmore,W.A. (2006) Disruption of Ledgf/Psip1 results in perinatal mortality and homeotic skeletal transformations. *Mol. Cell. Biol.*, **26**, 7201–7210.
17. Marshall,H.M., Ronen,K., Berry,C., Llano,M., Sutherland,H., Saenz,D., Bickmore,W., Poeschla,E. and Bushman,F.D. (2007) Role of PSIP1/LEDGF/p75 in lentiviral infectivity and integration targeting. *PLoS One*, **2**, e1340.
18. Schrijvers,R., De Rijck,J., Demeulemeester,J., Adachi,N., Vets,S., Ronen,K., Christ,F., Bushman,F.D., Debyser,Z. and Gijsbers,R. (2012) LEDGF/p75-independent HIV-1 replication demonstrates a role for HRP-2 and remains sensitive to inhibition by LEDGINs. *PLoS Pathog.*, **8**, e1002558.
19. Ciuffi,A., Llano,M., Poeschla,E., Hoffmann,C., Leipzig,J., Shinn,P., Ecker,J.R. and Bushman,F. (2005) A role for LEDGF/p75 in targeting HIV DNA integration. *Nat. Med.*, **11**, 1287–1289.
20. Llano,M., Vanegas,M., Hutchins,N., Thompson,D., Delgado,S. and Poeschla,E.M. (2006) Identification and characterization of the chromatin-binding domains of the HIV-1 integrase interactor LEDGF/p75. *J. Mol. Biol.*, **360**, 760–773.
21. Turlure,F., Maertens,G., Rahman,S., Cherepanov,P. and Engelman,A. (2006) A tripartite DNA-binding element, comprised of the nuclear localization signal and two AT-hook motifs, mediates the association of LEDGF/p75 with chromatin in vivo. *Nucleic Acids Res.*, **34**, 1653–1665.
22. Shun,M.C., Botbol,Y., Li,X., Di Nunzio,F., Daigle,J.E., Yan,N., Lieberman,J., Lavigne,M. and Engelman,A. (2008) Identification and characterization of PWWP domain residues critical for LEDGF/p75 chromatin binding and human immunodeficiency virus type 1 infectivity. *J. Virol.*, **82**, 11555–11567.
23. Cherepanov,P., Devroe,E., Silver,P.A. and Engelman,A. (2004) Identification of an evolutionarily conserved domain in human lens epithelium-derived growth factor/transcriptional co-activator p75 (LEDGF/p75) that binds HIV-1 integrase. *J. Biol. Chem.*, **279**, 48883–48892.
24. Vanegas,M., Llano,M., Delgado,S., Thompson,D., Peretz,M. and Poeschla,E. (2005) Identification of the LEDGF/p75 HIV-1 integrase-interaction domain and NLS reveals NLS-independent chromatin tethering. *J. Cell Sci.*, **118**, 1733–1743.
25. Cherepanov,P. (2007) LEDGF/p75 interacts with divergent lentiviral integrases and modulates their enzymatic activity in vitro. *Nucleic Acids Res.*, **35**, 113–124.
26. Izumoto,Y., Kuroda,T., Harada,H., Kishimoto,T. and Nakamura,H. (1997) Hepatoma-derived growth factor belongs to a gene family in mice showing significant homology in the amino terminus. *Biochem. Biophys. Res. Commun.*, **238**, 26–32.
27. Vandegraaff,N., Devroe,E., Turlure,F., Silver,P.A. and Engelman,A. (2006) Biochemical and genetic analyses of integrase-interacting proteins lens epithelium-derived growth factor (LEDGF)/p75 and hepatoma-derived growth factor related protein 2 (HRP2) in preintegration complex function and HIV-1 replication. *Virology*, **346**, 415–426.
28. Fenwick,C.W., Tremblay,S., Wardrop,E., Bethell,R., Coulomb,R., Elston,R., Faucher,A.-M., Mason,S., Simoneau,B., Tsantrizos,Y. *et al.* (2011) Resistance studies with HIV-1 non-catalytic site integrase inhibitors. *Antiviral Ther.*, **16(Suppl. 1)**, A9.
29. Tsantrizos,Y.S., Bailey,M.D., Bilodeau,F., Carson,R.J., Coulombe,R., Fader,L., Halmos,T., Kawai,S., Landry,S., Laplante,S. *et al.* (2009), World Patent WO 2009/062285 A1.
30. Li,X., Koh,Y. and Engelman,A. (2012) Correlation of recombinant integrase activity and functional preintegration complex formation during acute infection by replication-defective integrase mutant human immunodeficiency virus. *J. Virol.*, **86**, 3861–3879.
31. Shun,M.C., Daigle,J.E., Vandegraaff,N. and Engelman,A. (2007) Wild-type levels of human immunodeficiency virus type 1 infectivity in the absence of cellular emerin protein. *J. Virol.*, **81**, 166–172.
32. Koh,Y., Haim,H. and Engelman,A. (2011) Identification and characterization of persistent intracellular human immunodeficiency virus type 1 integrase strand transfer inhibitor activity. *Antimicrob. Agents Chemother.*, **55**, 42–49.
33. Julias,J.G., Ferris,A.L., Boyer,P.L. and Hughes,S.H. (2001) Replication of phenotypically mixed human immunodeficiency virus type 1 virions containing catalytically active and catalytically inactive reverse transcriptase. *J. Virol.*, **75**, 6537–6546.
34. Butler,S.L., Hansen,M.S. and Bushman,F.D. (2001) A quantitative assay for HIV DNA integration in vivo. *Nat. Med.*, **7**, 631–634.
35. Matreyek,K.A. and Engelman,A. (2011) The requirement for nucleoporin NUP153 during human immunodeficiency virus type 1 infection is determined by the viral capsid. *J. Virol.*, **85**, 7818–7827.
36. Gillet,N.A., Malani,N., Melamed,A., Gormley,N., Carter,R., Bentley,D., Berry,C., Bushman,F.D., Taylor,G.P. and Bangham,C.R.M. (2011) The host genomic environment of the provirus determines the abundance of HTLV-1–infected T-cell clones. *Blood*, **117**, 3113–3122.
37. Ferris,A.L., Wu,X., Hughes,C.M., Stewart,C., Smith,S.J., Milne,T.A., Wang,G.G., Shun,M.C., Allis,C.D., Engelman,A. *et al.* (2010) Lens epithelium-derived growth factor fusion proteins redirect HIV-1 DNA integration. *Proc. Natl Acad. Sci. USA*, **107**, 3135–3140.

38. Cherepanov,P., Sun,Z.Y., Rahman,S., Maertens,G., Wagner,G. and Engelman,A. (2005) Solution structure of the HIV-1 integrase-binding domain in LEDGF/p75. *Nat. Struct. Mol. Biol.*, **12**, 526–532.
39. Stryke,D., Kawamoto,M., Huang,C.C., Johns,S.J., King,L.A., Harper,C.A., Meng,E.C., Lee,R.E., Yee,A., L'Italien,L. *et al.* (2003) BayGenomics: a resource of insertional mutations in mouse embryonic stem cells. *Nucleic Acids Res.*, **31**, 278–281.
40. McClive,P., Pall,G., Newton,K., Lee,M., Mullins,J. and Forrester,L. (1998) Gene trap integrations expressed in the developing heart: insertion site affects splicing of the PT1-ATG vector. *Dev. Dyn.*, **212**, 267–276.
41. Salmon,N.A., Reijo Pera,R.A. and Xu,E.Y. (2006) A gene trap knockout of the abundant sperm tail protein, outer dense fiber 2, results in preimplantation lethality. *Genesis*, **44**, 515–522.
42. Nakajima,N., Lu,R. and Engelman,A. (2001) Human immunodeficiency virus type 1 replication in the absence of integrase-mediated DNA recombination: definition of permissive and nonpermissive T-cell lines. *J. Virol.*, **75**, 7944–7955.
43. Wu,Y. and Marsh,J.W. (2003) Early transcription from nonintegrated DNA in human immunodeficiency virus infection. *J. Virol.*, **77**, 10376–10382.
44. Llano,M., Vanegas,M., Fregoso,O., Saenz,D., Chung,S., Peretz,M. and Poeschla,E.M. (2004) LEDGF/p75 determines cellular trafficking of diverse lentiviral but not murine oncoretroviral integrase proteins and is a component of functional lentiviral preintegration complexes. *J. Virol.*, **78**, 9524–9537.
45. Busschots,K., Vercammen,J., Emiliani,S., Benarous,R., Engelborghs,Y., Christ,F. and Debyser,Z. (2005) The interaction of LEDGF/p75 with integrase is lentivirus-specific and promotes DNA binding. *J. Biol. Chem.*, **280**, 17841–17847.
46. Hazuda,D.J., Felock,P., Witmer,M., Wolfe,A., Stillmock,K., Grobler,J.A., Espeseth,A., Gabryelski,L., Schleif,W., Blau,C. *et al.* (2000) Inhibitors of strand transfer that prevent integration and inhibit HIV-1 replication in cells. *Science*, **287**, 646–650.
47. Ocwieja,K.E., Brady,T.L., Ronen,K., Huegel,A., Roth,S.L., Schaller,T., James,L.C., Towers,G.J., Young,J.A., Chanda,S.K. *et al.* (2011) HIV integration targeting: a pathway involving Transportin-3 and the nuclear pore protein RanBP2. *PLoS Pathog.*, **7**, e1001313.
48. Holman,A.G. and Coffin,J.M. (2005) Symmetrical base preferences surrounding HIV-1, avian sarcoma/leukosis virus, and murine leukemia virus integration sites. *Proc. Natl Acad. Sci. USA*, **102**, 6103–6107.
49. Cherepanov,P., Ambrosio,A.L.B., Rahman,S., Ellenberger,T. and Engelman,A. (2005) From the Cover: structural basis for the recognition between HIV-1 integrase and transcriptional coactivator p75. *Proc. Natl Acad. Sci. USA*, **102**, 17308–17313.
50. Christ,F., Voet,A., Marchand,A., Nicolet,S., Desimmie,B.A., Marchand,D., Bardiot,D., Van der Veken,N.J., Van Remoortel,B., Strelkov,S.V. *et al.* (2010) Rational design of small-molecule inhibitors of the LEDGF/p75-integrase interaction and HIV replication. *Nat. Chem. Biol.*, **6**, 442–448.
51. Kessl,J.J., Jena,N., Koh,Y., Taskent-Sezgin,H., Slaughter,A., Feng,L., de Silva,S., Wu,L., Le Grice,S.F.J., Engelman,A. *et al.* (2012) Multimode, cooperative mechanism of action of allosteric HIV-1 integrase inhibitors. *J. Biol. Chem.*, **287**, 16801–16811.
52. Tsiang,M., Jones,G.S., Niedziela-Majka,A., Kan,E., Lansdon,E.B., Huang,W., Hung,M., Samuel,D., Novikov,N., Xu,Y. *et al.* (2012) New class of HIV-1 integrase (IN) inhibitors with a dual mode of action. *J. Biol. Chem.*, **287**, 21189–21203.
53. Christ,F., Shaw,S., Demeulemeester,J., Desimmie,B.A., Marchand,A., Butler,S., Smets,W., Chaltin,P., Westby,M., Debyser,Z. *et al.* (2012) Small molecule inhibitors of the LEDGF/p75 binding site of integrase (LEDGINs) block HIV replication and modulate integrase multimerization. *Antimicrob. Agents Chemother.*, **56**, 4365–4374.
54. Bieniasz,P.D. and Cullen,B.R. (2000) Multiple blocks to human immunodeficiency virus type 1 replication in rodent cells. *J. Virol.*, **74**, 9868–9877.
55. Siva,A.C. and Bushman,F. (2002) Poly(ADP-Ribose) polymerase 1 is not strictly required for infection of murine cells by retroviruses. *J. Virol.*, **76**, 11904–11910.
56. Ariumi,Y., Turelli,P., Masutani,M. and Trono,D. (2005) DNA damage sensors ATM, ATR, DNA-PKcs, and PARP-1 are dispensable for human immunodeficiency virus type 1 integration. *J. Virol.*, **79**, 2973–2978.
57. Mulky,A., Cohen,T.V., Kozlov,S.V., Korbei,B., Foisner,R., Stewart,C.L. and KewalRamani,V.N. (2008) The LEM domain proteins emerin and LAP2α are dispensable for human immunodeficiency virus type 1 and murine leukemia virus infections. *J. Virol.*, **82**, 5860–5868.
58. McKee,C.J., Kessl,J.J., Shkriabai,N., Dar,M.J., Engelman,A. and Kvaratskhelia,M. (2008) Dynamic modulation of HIV-1 integrase structure and function by cellular lens epithelium-derived growth factor (LEDGF) protein. *J. Biol. Chem.*, **283**, 31802–31812.
59. Hare,S., Di Nunzio,F., Labeja,A., Wang,J., Engelman,A. and Cherepanov,P. (2009) Structural basis for functional tetramerization of lentiviral integrase. *PLoS Pathog.*, **5**, e1000515.
60. Hare,S., Shun,M.C., Gupta,S.S., Valkov,E., Engelman,A. and Cherepanov,P. (2009) A novel co-crystal structure affords the design of gain-of-function lentiviral integrase mutants in the presence of modified PSIP1/LEDGF/p75. *PLoS Pathog.*, **5**, e1000259.
61. Kessl,J.J., Li,M., Ignatov,M., Shkriabai,N., Eidahl,J.O., Feng,L., Musier-Forsyth,K., Craigie,R. and Kvaratskhelia,M. (2011) FRET analysis reveals distinct conformations of IN tetramers in the presence of viral DNA or LEDGF/p75. *Nucleic Acids Res.*, **39**, 9009–9022.
62. Raghavendra,N.K. and Engelman,A. (2007) LEDGF/p75 interferes with the formation of synaptic nucleoprotein complexes that catalyze full-site HIV-1 DNA integration in vitro: implications for the mechanism of viral cDNA integration. *Virology*, **360**, 1–5.
63. Shen,L., Rabi,S.A. and Siliciano,R.F. (2009) A novel method for determining the inhibitory potential of anti-HIV drugs. *Trends Pharmacol. Sci.*, **30**, 610–616.
64. De Rijck,J., Vandekerckhove,L., Gijsbers,R., Hombrouck,A., Hendrix,J., Vercammen,J., Engelborghs,Y., Christ,F. and Debyser,Z. (2006) Overexpression of the lens epithelium-derived growth factor/p75 integrase binding domain inhibits human immunodeficiency virus replication. *J. Virol.*, **80**, 11498–11509.
65. Benkhelifa-Ziyyat,S., Bucher,S., Zanta-Boussif,M.A., Pasquet,J. and Danos,O. (2010) Changes in the accessibility of the HIV-1 integrase C-terminus in the presence of cellular proteins. *Retrovirology*, **7**, 27.
66. Wolkenberg,S.E., Zhao,Z., Thut,C., Maxwell,J.W., McDonald,T.P., Kinose,F., Reilly,M., Lindsley,C.W. and Hartman,G.D. (2011) Design, synthesis, and evaluation of novel 3,6-diaryl-4-aminoalkoxyquinolines as selective agonists of somatostatin receptor subtype 2. *J. Med. Chem.*, **54**, 2351–2358.
67. Devita,R.J., Chang,L., Hoang,M.T., Jiang,J., Lin,P. and Sailer,A.W. (2003) International Patent Application WO 03/045920 A1.
68. Ho,G.D., Seganish,W.M., Tulshian,D.B., Timmers,C.M., Rijn,R.D.V. and Loozen,H.J.J. (2011) International Patent Application WO 2011/008597 A1.
69. Beaulieu,P.L., Edwards,P.J., Poirier,M., Racourt,J. and Stammers,T.A. (2009) International Patent Application WO 2009/018657 A1.
70. Corey,E.J. and Schmidt,G. (1979) Useful procedures for the oxidation of alcohols involving pyridinium dichromate in approtic media. *Tet. Lett.*, **20**, 399–402.